Molecular Cloning and Characterization of a Candidate Human Growth-Related and Time-Keeping Constitutive Cell Surface Hydroquinone (NADH) Oxidase

Ziying Jiang,[‡] Nina M. Gorenstein,[§] Dorothy M. Morré,[‡] and D. James Morré*,[||]

Departments of Foods and Nutrition, Biological Sciences, and Medicinal Chemistry and Molecular Pharmacology, Purdue University, West Lafayette, Indiana 47907

Received June 6, 2008; Revised Manuscript Received September 5, 2008

ABSTRACT: ENOX (ECTO-NOX) proteins are growth-related cell surface proteins that catalyze both hydroquinone or NADH oxidation and protein disulfide−thiol interchange and exhibit both prion-like and time-keeping (clock) properties. The two enzymatic activities they catalyze alternate to generate a regular period of 24 min in length. Here we report the cloning, expression, and characterization of a human candidate constitutive ENOX (CNOX or ENOX1) protein. The gene encoding this 643 amino acid long protein is located on chromosome 13 (13q 14.11). Functional motifs previously identified by site-directed mutagenesis in a cancer-associated ENOX (tNOX or ENOX2) as adenine nucleotide or copper binding along with essential cysteines are present, but the drug-binding motif (EEMTE) sequence of ENOX2 is absent. The activities of the recombinant protein expressed in *Escherichia coli* were not affected by capsaicin, EGCg, and other ENOX2-inhibiting substances. The purified recombinant protein bound ca. 2 mol of copper/mol of protein. Bound copper was necessary for activity. H260 and H579 were required for copper binding as confirmed by site-directed mutagenesis, loss of copper-binding capacity, and resultant loss of enzymatic activity. Addition of melatonin phased the 24 min period such that the next complete period began exactly 24 min after the melatonin addition as appears to be characteristic of ENOX1 activities in general. Oxidative activity was exhibited with both NAD(P)H and reduced coenzyme Q as substrate. Concentrated solutions of the purified candidate ENOX1 protein irreversibly formed insoluble aggregates, devoid of enzymatic activity, resembling amyloid.

All animals and plants thus far investigated exhibit one or more hormone-responsive external plasma membrane hydroquinone oxidases capable of catalyzing protein disulfide interchange and that oxidize NAD(P)H as an alternate substrate (NADH oxidase = NOX) (*1, 2*). Based on activity characteristics, three related but distinct ECTO-NOX or ENOX[1] (for external cell surface NOX) proteins have been reported. One (CNOX or ENOX1) is constitutive with an activity that is widely distributed among animals, plants, and yeast. A second ENOX activity is tumor- or cancer-associated, designated tNOX or ENOX2. ENOX2 proteins are inhibited by a series of quinone site inhibitors, all with anticancer activity including the vanilloid, capsaicin (*3, 4*), and the antitumor sulfonylurea LY181984 (*5*). Shed forms of both activities are found in culture media conditioned by the growth of mammalian or plant cells (*6*). A 33.5 kDa protein with capsaicin-inhibited NADH oxidase activity was purified from spent media of cultured HeLa cells (*7*) and from sera of cancer patients (*8*). The NADH activities from sera of healthy volunteers or spent media of noncancer cells were unaffected by ENOX2 inhibitors (*9*).

Sera of cancer patients and plasma membranes of cancer cell lines grown in culture contained both ENOX1 and ENOX2 (*2, 10*). ENOX1 is found with noncancer cells and sera of healthy volunteers or of patients with diseases other than cancer which lack ENOX2 (*11*). A third protein with ENOX-like activity (designated arNOX) is age-related (*12*) and evident only in aged individuals, late passage cultured cells, or senescent plant parts (*12, 13*).

The ENOX1 and ENOX2 proteins function in the cell enlargement phase of cell growth (*14*−*16*). When their activity is inhibited, cells are unable to enlarge (*2, 3, 17, 18*). Cancer cells in culture when inhibited either by capsaicin (*3*) or by other antitumor drugs (*1, 5*) are unable to enlarge to a size sufficient to allow division and undergo apoptosis. *Arabidopsis* seedlings treated with the quassinoid ENOX1 inhibitor simalikalactone D ceased growth until the drug was metabolized but did not die (*18*).

A distinguishing characteristic of ENOX proteins that permits their unequivocal identification is that the proteins exhibit two activities that alternate (*1, 2*). The first activity is that of a hydroquinone oxidase (NADH serves as an alternate substrate for this activity) (*19*). The second is that

* To whom correspondence should be addressed. Phone: 765-494-1388. Fax: 765-494-4007. E-mail: morre@pharmacy.purdue.edu.

[‡] Department of Foods and Nutrition, Purdue University.

[§] Department of Biological Sciences, Purdue University.

[||] Department of Medicinal Chemistry and Molecular Pharmacology, Purdue University.

[1] Abbreviations: CNOX, constitutive and drug-unresponsive cell surface NADH oxidase (ENOX1); cENOX1, candidate ENOX1; capsaicin, 8-methyl-*N*-vanillyl-6-noneamide; EGCg, (−)-epigallocatechin-3-gallate; ENOX, ECTO-NOX; mPMS, 1-methoxy-5-methylphenazinium methyl sulfate; NBT, nitro blue tetrazolium; tNOX, tumor- (cancer-) associated and drug- (capsaicin-) inhibited cell surface NADH oxidase (ENOX2); SDS−PAGE, sodium dodecyl sulfate−polyacrylamide gel electrophoresis; IEF, isoelectric focusing; MBP, maltose binding protein; WST-1, 2-(4-iodophenyl)-3-(4-nitrophenyl)-5-(2,4-disulfophenyl)-2*H*-tetrazolium monosodium salt.

10.1021/bi801073p CCC: $40.75
Published on Web 12/04/2008

of a protein disulfide−thiol interchange measured either from the restoration of activity to inactive (scrambled) RNase (*20*) or from the cleavage of dithiodipyridine substrates (*21*). Each activity generates a distinct oscillatory activity with a period length of 24 min for ENOX1. The strictly periodic activity of the NOX proteins (ENOX1 and ENOX2 as well as arNOX) distinguishes their activity from all other oxidase or protein disulfide isomerase forms (*22*) and imparts to the ENOX1 protein a potential role as an ultradian (with period lengths of less than 24 h) oscillator of the cellular biological clock (*23*).

In a previous report (*11*), purification of a protease-resistant protein fragment with drug-resistant ENOX1 activity and a period length of 24 min from human serum protein was described. The protein fragment was blocked to direct sequencing and was resistant to further protease digestion. Polyclonal antibodies raised to the fragment partially blocked total NOX activity of human sera and from the surface of human noncancer cells but did not react with recombinant ENOX2 or with molecular species identified as ENOX2 from sera of cancer patients or from cancer cell lines grown in culture. These antibodies inhibited the activity of the protein reported here and have aided in its identification as the first candidate ENOX1 to be cloned and expressed as a recombinant protein.

ENOX proteins lack iron or iron−sulfur clusters but still reduce oxygen. The previously cloned and sequenced ENOX2 protein contains a copper site conserved with the copper site of the enzyme Mg^{2+} superoxide dismutase (*22*). Site-directed mutagenesis of this copper site resulted in the loss of enzymatic activity when the mutant protein was expressed in *Escherichia coli* (*22, 24*). These findings were extended to the candidate ENOX1 protein with the discovery of a second copper site also required for activity. These findings raise the possibility that the concerted four electron transfers required to reduce molecular oxygen to water are carried out by dimers of the dicopper-containing ENOX monomers.

METHODS

Search for Candidate Constitutive ENOX1 (cENOX1). Protein BLAST (Basic Local Alignment Search Tool) with ENOX2 sequence as a query was used for similarity searches in different databases (nonredundant protein sequences, UniProt, EST, and others) (*25*). The protein product of the human proliferation-inducing gene 38 was selected for evaluation as a candidate constitutive ENOX1.

Cloning of Candidate ENOX1 (cENOX1). mRNA was extracted from 5×10^6 HeLa cells using a Oligotex Direct mRNA Micro Kit (QIAGEN, Valencia, CA), and cDNA was synthesized by reverse transcription PCR using M-MLV reverse transcriptase (Promega) and oligo$(dT)_{15}$ (Promega, Madison, WI) as a primer. The open reading frame of cENOX1 was then amplified using *Pfu* Turbo DNA polymerase (Stratagene, La Jolla, CA) and two primers: 5′-ATTTATCCGCGGGTATGGTAGATGCAGGTGGAG-3′ (forward) and 5′-AGCTGGCGCGCCTTAGGTAGTTTTAATTCC-3′ (reverse). The amplified fragment was digested with restriction endonucleases *Asc*I and *Sac*II (New England Biolabs, Ipswich, MA) and ligated into *Asc*I and *Sac*II sites of the pET-43.1a vector (Novagen, Madison, WI) using T4 DNA ligase (New England Biolabs, Ipswich, MA). This construct allowed for expression of cENOX1 as a NusA-His_6 fusion protein. The second construct was designed for expression of cENOX1 as a fusion protein with a removable maltose binding protein (MBP) tag. A cleavage site ENLYFQG of the protease of tobacco etch virus (TEV) was introduced between MBP and cENOX1 sequences. For this construct, the open reading frame of cENOX1 was amplified by PCR using primers 5′-TGGATCCGAAAATTTATATTTTCAGGGCGGTATGGTAGATGCAGGTGGAGTT-3′ (forward) and 5′-ATTGTCGACTTAGGTAGTTTTAATTCCTTCAAAGGC-3′ (reverse). The amplified fragment was digested with restriction endonucleases *Bam*HI and *Sal*I (New England Biolabs, Ipswich, MA) and ligated into *Bam*HI and *Sal*I sites of the pMAL-c2E vector (New England Biolabs). After purification of the plasmid DNA from *E. coli* cells (DH5α) with the QIAGEN plasmid midi kit (QIAGEN), selected clones were sequenced.

Site-Directed Mutagenesis of Putative Copper-Binding Sites in cENOX1. Two sets of oligonucleotides were designed to replace amino acid residues involved in each potential copper-binding site of cENOX1 by site-directed mutagenesis. The potential copper-binding sites were HCKSC120, H260YSEH, Y304SM, H531SH, H579VH, and M608LLM. The primer pairs designed to replace the numbered amino acids by alanine are as follows: C120A, 5′-CAAAGAAATAATCCACTGCAAAAGCGCTACTCTTTTTCCTCAAAATCCAAAT-3′ (forward) and 5′-ATTTGGATTTTGAGGAAAAAGAGTAGCGCTTTTGCAGTGGATTATTTCTTTG-3′ (reverse); H260A, 5′-CCCGCCTGCCATAATGGCCTACTCGGAGCACG-3′ (forward) and 5′-CGTGCTCCGAGTAGGCCATTATGGCAGGCGGG-3′ (reverse); Y304A, 5′-GCTCTGCAAACCAGTTCGCTTCCATGGTGCAGTCGG-3′ (forward) and 5′-CCGACTGCACCATGGAAGCGAACTGGTTTGCAGAGC-3′ (reverse); H531A, 5′-GGTCGAGACCAATGGCGCCAGCCATGAGGATTCA-3′ (forward) and 5′-TGAATCCTCATGGCTGGCGCCATTGGTCTCGACC-3′ (reverse); H579A, 5′-GCTAATAGGTATCATATCAAGCTTTCTTGCCGTCCATCCTTTTGG-3′ (forward) and 5′-GCTAATAGGTATCATATCAACGTTTCTTGCCGTCCATCCTTTTGG-3′ (reverse); M608A, 5′-CAAGATATCTGCAAATGAAATAGAAGCGCTTTTGATGAGGCTGCCAC-3′ (forward) and 5′-GTGGCAGCCTCATCAAAAGCGCTTCTATTTCATTTGCAGATATCTTG-3′ (reverse).

The plasmid pMAL-c2E-cENOX1 and mutagenic primers were combined in a 50 μL reaction mixture containing deoxyribonucleotides, buffer, and high fidelity *Pfu* DNA polymerase according to the manufacturer's protocol of the QuikChange II XL site-directed mutagenesis kit (Stratagene, La Jolla, CA). Low cycle number was used to minimize unwanted second site mutations. The linear amplification product was treated with endonuclease *Dpn*I (10 units/μL) for 1 h to eliminate the parental template. For the H260A and H579A double mutant of MBP-tagged cENOX1, the H579A plasmid and the H260A mutagenic primer pairs were used in the PCR reaction. Other steps were as described above. The reaction mixture was transformed into XL10-Gold unltracompetent cells. DNA sequencing was utilized to confirm the correct replacement.

Expression of Recombinant cENOX1. Both native constructs as well as mutant forms of MBP-tagged cENOX1

protein were expressed similarly. *E. coli* competent cells BL21(DE3) (Novagen, Madison, WI) were transformed with a prepared expression vector. For expression of NusA-fused protein, cells were grown at 37 °C in LB medium containing ampicillin (100 μg/mL) for 10 h, induced with IPTG (to 1 mM final concentration), and grown overnight. Cells were harvested by centrifugation at 4000*g* for 15 min. For expression of MBP-tagged cENOX1 (either native or mutant), cells were grown in 10 mL of TB medium containing ampicillin (100 μg/mL) overnight, diluted 1:100, grown for an additional 3 h, induced with IPTG (0.3 mM final concentration), and grown for 3 h before harvesting.

Purification. Cells with NusA-tagged cENOX1 were resuspended in 20 mM Tris-HCl, pH 7.5, containing 0.5 mM PMSF, 1 mM EDTA, 1 mM benzamidine, and 1 mM 6-aminocaproic acid (buffer A). Cells were lysed by three passages through a French pressure cell (SLM Aminco) at 20000 psi. The lysate was centrifuged at 5000*g*, and the NusA-fused cENOX1 was purified from the supernatant using a Ni-NTA Superflow nickel-charged resin (QIAGEN) column according to the manufacturer's protocol. For isolation of MBP-tagged cENOX1, cells were resuspended in buffer A (above), lysed as above, and purified with an amylose resin column (New England Biolabs) according to the manufacturer's protocol. Expression and purification of all forms of cENOX1 were confirmed by SDS−PAGE with silver staining.

Isoelectric Focusing (IEF) Gel Slicing. The fusion cENOX1 proteins were further purified from partially purified mixtures on Criterion IEF gels (Bio-Rad, Hercules, CA). The IEF gel was cut at p*I*s of 7.0, 6.0, and 4.5 based on IEF standards (Bio-Rad). The slices were soaked in 15 mM Tris−Mes buffer, pH 7, at 4 °C for overnight. The gel-free extracts were assayed for ENOX1 activity. The molecular masses of the extracted proteins from the slices were evaluated by SDS−PAGE with silver staining. Protein concentrations were determined by the bicinchoninic acid (BCA) method (*26*) with bovine serum albumin as a control.

Removal of the MBP Tag from Recombinant cENOX1. AcTEV protease (Invitrogen, Carlsbad, CA) equivalent to 1000 units was added to 4 mg of affinity purified MBP-tagged cENOX1 in a total volume of 20 mL and incubated at 30 °C for 1 h. cENOX1 pellet with the tag removed was obtained by centrifugation (Beckman Optima LE-80K, rotor SW28, 112700*g*, 4 °C).

Enzyme Activity Assays. Oxidation of NADH was determined spectrophotometrically from the disappearance of NADH measured at 340 nm in a reaction mixture containing 25 mM Tris−MES (pH 7.2), 100 μM GSH, 1 mM KCN to inhibit mitochondrial oxidase activity, 150 μM NADH, and the enzyme at 37 °C with temperature control (±0.5 °C) and stirring. Prior to assay, 1 μM reduced glutathione was added to reduce the protein in the presence of substrate. After 10 min, 0.03% hydrogen peroxide was added to reoxidize the protein under renaturing conditions and in the presence of substrate to start the reaction. Activities were measured using paired Hitachi U3210 spectrophotometers with continuous recording. Assays were for 1 min and were repeated on the same sample at intervals of 1.5 min for the times indicated. An extinction coefficient of 6.22 mM^{-1} cm^{-1} was used to determine specific activity.

Oxidation of reduced coenzyme Q_{10} ($CoQ_{10}H_2$) was measured as the disappearance of reduced CoQ at both 290 and 410 nM (*19*). The method for preparation of reduced coenzyme Qs (50 mM coenzyme Q_0 stock solution or 7.5 mM coenzyme Q_{10} stock solution in ethanol) involved addition of an equal volume of 0.25% $NaBH_4$ under nitrogen followed after several minutes by 0.1 volume of 0.1 N HC1 to degrade the excess $NaBH_4$. The reduced coenzyme Q_{10} was prepared fresh for each experiment. For oxidation of $Q_{10}H_2$ the reaction mixture contained the enzyme source in 2.5 mL of 50 mM Tris−MES buffer, pH 7.0. Triton X-100 (0.08%) was used to solubilize the $Q_{10}H_2$ in the assay buffer. The reaction was started with the addition of 40 μL of 5 mM $Q_{10}H_2$. An extinction coefficient of 0.805 mM^{-1} cm^{-1} was used to calculate the rate of $Q_{10}H_2$ oxidation.

Protein disulfide−thiol interchange was determined either by restoration of activity to scrambled and inactive ribonuclease (RNase) prepared from native RNase A as described with cCMP as the RNase substrate or by spectrophotometry from the increase in absorbance at 340 nm resulting from the cleavage of dithiodipyridine (DTDP) (*21*).

RNase A activity was assayed by incubating inactive, oxidized, and scrambled RNase A together with 50 mM Tris−MES buffer (pH 6.0), 0.45 mM cCMP, 1 μM GSH or GSSG or GSH plus GSSG, and IEF-purified cENOX1 proteins. Hydrolysis of cCMP resulting from the activation of the initially randomly oxidized and inactive RNase was recorded continuously as an increase in A_{296} resulting from cCMP hydrolysis (extinction coefficient = 0.19 mM^{-1} cm^{-1}).

DTDP cleavage was buffered (50 mM) in Tris−MES at pH 7. The assay was preincubated with 0.5 μmol of 2,2′-dithiodipyridine (DTDP) in 5 μL of DMSO to react with endogenous reductants present with the plasma membranes. After 10 min, a further 3.5 μmol of DTDP were added in 35 μL of DMSO to start the reaction. The final reaction volume was 2.5 mL. The reaction was monitored from the increase in absorbance at 340 nm. Specific activities were calculated using a millimolar absorption coefficient of 6.21.

Proteins were estimated by the bicinchoninic acid method (*26*). Bovine serum albumin was the standard.

Removal of Copper(II) from Fusion of cENOX1. Purified MBP-tagged cENOX1 was concentrated to 0.7 mg/mL by using a Centricon concentrator (Millipore Corp., Danvers, MA) fitted with a 10000 nominal molecular weight limit ultracel YM membrane. Samples (500 μL) were combined with 1 μL of trifluoroacetic acid (TFA) in the presence or absence of 15 μL of 10 mM bathocuproine. After 2 h of incubation at room temperature, the samples were dialyzed (Spectra/Por dialysis membrane, molecular weight cutoff 6000−8000; Spectrum Laboratories, Rancho Dominquez, CA) against 15 mM Tris−Mes, pH 7, at 4 °C for two changes of 8 h each. The samples then were concentrated to 250 μL for Criterion IEF gel electrophoretic fractionation and subsequent elution as above.

Determination of Copper(II) in cENOX1 and Mutant Proteins. The copper amounts of purified MBP-tagged protein, MBP-tagged cENOX1 protein, and mutant proteins, including H260A, H579A, and H260A, H579A double mutant MBP-tagged proteins, were determined by a colorimetric assay. To 100 μL protein (ca. 10 μM) samples were added 25 μL of 0.3 g/mL trichloroacetic acid, 20 μL of 0.35 mg/mL L-dehydroascorbic acid, and 160 μL of 0.067 mg/

mL disodium bicinchoninic acid containing 0.04 mg/mL NaOH and 0.17 mg/mL HEPES sodium salt. The mixture was incubated at room temperature overnight. Distilled water (2 mL) then was added, and the absorbance values were recorded at 354 nm. The copper contents were estimated from a standard copper series from 5 to 30 μM assayed in parallel (*27*).

Electron Microscopy. For electron miscroscopy, an aqueous solution of IEF-purified and concentrated NusA-tagged cENOX1 was mixed with an equal volume of 17% uranyl acetate on glow-discharged Formvar-coated electron microscope grids. Negatively stained samples were imaged using a Philips CM-100 TEM operated at 100 bv, spot 3, 200 μM condenser aperture, and 70 μM objective aperture. Images were captured on Kodak SO-163 electron image film. The primary magnifications were 39000×.

RESULTS

The Protein BLAST search with the ENOX2 sequence as the query identified the protein product of the proliferation-inducing gene protein 38 as a candidate ENOX1 (cENOX1). The two sequences were 64% identical. In the human genome, the gene is located on chromosome 13 (13q 14.11) (*28*). The sequence included a NADH-binding site, a disulfide−thiol interchange site, and potential copper-binding sites similar to those of ENOX2 but excluded the anticancer EEMTE drug-binding site of ENOX2.

Cloning. The full-length cENOX1 was cloned from a HeLa cDNA library and inserted into the vector pET43.1a for expression of a fused protein with NusA and His tags. The sequencing of the construct yielded an insert of 1929 bp that encoded an open reading frame of 643 amino acids (Figure 1). The full-length cENOX1 was recloned into the vector pMAL-c2E using the construct pET43.1a-cENOX1 as a template for PCR amplification of the gene. Sequencing of two clones of pET43.1a-cENOX1 revealed a new isoform having a semiconserved mutation of E16 to D. Protein, purified from the pMAL-c2E-cENOX1 construct, contained two mutations (I94 to T and R249 to W) introduced during PCR amplification. The originally amplified sequence (without mutation) was submitted to NCBI GenBank with an assigned accession number of EF432052.

Protein Characterization. A continuous trace of an IEF-purified preparation of recombinant MBP-tagged cENOX2 illustrates the oscillatory activity characteristic of the ENOX proteins (Figure 2). Intervals of rapid activity (arrows) were interspersed with intervals of less activity. The period length was 24 min. No oscillations were observed with NADH alone or with cENOX1 in the absence of NADH.

For more detailed evaluations, rates averaged over 1 min every 1.5 min with recombinant cENOX1 expressed in bacteria exhibited more clearly the oscillatory pattern of oxidation of exogenously supplied NADH characteristic of ENOX proteins (Figure 3A). The repeating pattern was that of five maxima, two of which were separated by 6 min (arrows) and the remainder separated by 4.5 min ($6 + 4 \times 4.5 = 24$ min). As is characteristic of ENOX1 proteins from other sources, the oscillatory pattern could be phased by the addition of 1 μM melatonin (Figure 3B). A new maximum was observed 24 min after melatonin addition.

That the activity was not that of ENOX2 was shown by resistance of the activity to inhibition by the active pungent principle of chili peppers, capsaicin (8-methyl-*N*-vanillyl-6-noneamide). In the presence or absence of 1 μM capsaicin, a concentration sufficient to inhibit ENOX2 completely, the activity was unaffected (Figure 3C,D).

A third criterion to identify the expressed protein as an ENOX1 was inhibition of the activity by a ENOX1-specific antibody raised against the circulating form of ENOX1 from human sera (Figure 3E,F). As is typical of antibody inhibition of ENOX activity, inhibition was delayed through approximately one full cycle of activity to permit antibody binding after which the activity ceased (Figure 3F). In the absence of antibody, the activity continued (Figure 3E).

As is characteristic of ENOX proteins in general, the proteins also exhibit protein disulfide−thiol interchange (protein disulfide isomerase) activity illustrated by the time-dependent restoration of activity to inactive, scrambled ribonuclease in a standard protein disulfide isomerase assay (Figure 4A). As reported previously (*2*), the two activities, NADH oxidation and protein disulfide interchange, alternate such that the activation of inactive, scrambled ribonuclease also is periodic. Similar results were obtained with the cleavage of a dithiodipyridyl substrate (Figure 4B). An oscillatory pattern similar to that for NADH oxidation was observed with a period length of 24 min (arrows).

The recombinant cENOX1 oxidized reduced coenzyme Q in a standard assay (Figure 5) with activity measured either at A_{410} (Figure 5A) or at A_{290} (Figure 5B). As with NADH oxidation (Figure 3A) and dithiodipyridine cleavage (Figure 4B), the characteristic pattern of oscillations with a 24 min period (arrows) was reproduced (Figure 5). Hydroquinones of the plasma membrane (reduced coenzyme Q for animals, reduced coenzyme Q or phylloquinone for plants) are the physiological substrates for ENOX proteins.

The ENOX activities of the recombinant proteins described above were restricted to proteins at the calculated molecular weight for NusA-tagged cENOX1 (Figure 6) by isoelectric focusing. All other proteins present in any of the preparations lacked these activities (Figure 6A). The material eluted from the isoelectric focusing gel exhibited the characteristic oscillatory pattern of ENOX proteins (Figure 6B) with a 24 min period (arrows), and the period was shifted by addition of melatonin based on phase at time of addition (Figure 6C) as is characteristic of ENOX1 (but not ENOX2) proteins. The new maxima occurred 24 min after melatonin addition and continued thereafter as phased by the melatonin addition. The ENOX activity eluted from the IEF gel was further identified as ENOX1 rather than ENOX2 by its resistance to various ENOX2 inhibitors including cis-platinum, phenoxodiol, EGCg, and capsaicin, all tested at concentrations sufficient to inhibit ENOX2 activity completely (Table 1). With the eluted ENOX from the IEF gels, no inhibition was observed. Activity was inhibited by the ENOX1-specific quassinoid inhibitor simalikalactone D.

cENOX1 Activity Requires the Presence of Copper. Copper presence was necessary for cENOX1 activity (Figure 7). The IEF-purified MBP-tagged cENOX1 when unfolded in the presence of trifluoroacetic acid retained activity after dialysis and at physiological pH (Figure 7A). However, if the cENOX1 was unfolded in the presence of the copper chelator bathocuproine, activity was lost (Figure 7B). Activity was subsequently restored by refolding in the presence of copper at physiological pH (Figure 7C).

```
ENOX2         1 --------MQRDFRWLWVYEIGYAADNSRTLNVDSTAMTLPMSDPTAWAT 42
cENOX1        1 MVDAGGVENITQLPQELPQMMAAAADGLGSIAIDTTQLNMSVTDPTAWAT 50
                          ::       :. ***.  :: :*:* :.:.::*******

ENOX2        43 AMNNLGMAPLGIAG------QPILPDFDPALGMMTGIPPITPMMPGLGIV 86
cENOX1       51 AMNNLGMVPVGLPGQQLVSDSICVPGFDPSLNMMTGITPINPMIPGLGLV 100
                *******.*:*:.*      .  :*.***:*.*****.**.**:****:*

ENOX2        87 PPPIPPDMPVVKEIIHCKSCTLFPPNPNLPPPATRERPPGCKTVFVGGLP 136
cENOX1      101 PPPPPTEVAVVKEIIHCKSCTLFPQNPNLPPPSTRERPPGCKTVFVGGLP 150
                *** *.:::.*************** *******:*****************

ENOX2       137 ENGTEQIIVEVFEQCGEIIAIRKSKKNFCHIRFAEEYMVDKALYLSGYRI 186
cENOX1      151 ENATEEIIQEVFEQCGDITAIRKSKKNFCHIRFAEEFMVDKAIYLSGYRM 200
                **.**:** *******:* *****************:*****:******:

ENOX2       187 RLGSSTDKKDTGRLHVDFAQARDDLYEWECKQRMLAREERHRRRMEEERL 236
cENOX1      201 RLGSSTDKKDSGRLHVDFAQARDDFYEWECKQRMRAREERHRRKLEEDRL 250
                **********:*************:********* ********::**:**

ENOX2       237 RPPSPPPVVHYSDHECSIVAEKLKDDSKFSEAVQTLLTWIERGEVNRRSA 286
cENOX1      251 RPPSPPAIMHYSEHEAALLAEKLKDDSKFSEAITVLLSWIERGEVNRRSA 300
                ******.::***:**.:::************: .**:************

ENOX2       287 NNFYSMIQSANSHVRRLVNEKAAHEKDMEEAKEKFKQALSGILIQFEQIV 336
cENOX1      301 NQFYSMVQSANSHVRRLMNEKATHEQEMEEAKENFKNALTGILTQFEQIV 350
                *:****:**********:****:**::******:**:**:*** ******

ENOX2       337 AVYHSASKQKAWDHFTKAQRKNISVWCKQAEEIRNIHNDELMGIRREEEM 386
cENOX1      351 AVFNASTRQKAWDHFSKAQRKNIDIWRKHSEELRNAQSEQLMGIRREEEM 400
                **:::::::*******:*******.:* *::**:** :.::**********

ENOX2       387 EMSDDE-IEEMTETKETEESALVSQAEALKEENDSLRWQLDAYRNEVELL 435
cENOX1      401 EMSDDENCDSPTKKMRVDESALAAQAYALKEENDSLRWQLDAYRNEVELL 450
                ******  :. *:. ..:****.:** **********************

ENOX2       436 KQEQGKVHREDD-PNKEQQLKLLQQALQGMQQHLLKVQEEYKKKEAELEK 484
cENOX1      451 KQEKEQLFRTEENLTKDQQLQFLQQTMQGMQQQLLTIQEELNNKKSELEQ 500
                ***: ::.* ::  .*:***::***::*****:**.:*** ::*::***:

ENOX2       485 LKDDKLQVEKMLENLKEKESCASRLCAS------------------NQD 515
cENOX1      501 AKEEQSHTQALLKVLQEQLKGTKELVETNGHSHEDSNEINVLTVALVNQD 550
                 *::: :.: :*: *:*: . :..*  :                  ***

ENOX2       516 SEYPLEKTMNSSPIKSEREALLVGIISTFLHVHPFGASIEYICSYLHRLD 565
cENOX1      551 RENNIEK--RSQGLKSEKEALLIGIISTFLHVHPFGANIEYLWSYMQQLD 598
                 *  +**  .*. :***:****:**********.***: **:::**

ENOX2       566 NKICTSDVECLMGRLQHTFKQEMTGVGASLEKRWKFCGFEGLKLT      610
cENOX1      599 SKISANEIEMLLMRLPRMFKQEFTGVGATLEKRWKLCAFEGIKTT      643
                .**.:.::* *: ** : ****:*****:******:*.***:* *
```

FIGURE 1: cENOX1 sequence and comparison to ENOX2. The drug-binding site underlined is present in ENOX2 but not in cENOX1. The NADH-binding sequences denoted by a dashed underline and the copper-binding sites denoted by dotted underlines are present in both ENOX2 and cENOX1. The C117XXC putative half of the protein disulfide interchange motif is indicated by closely spaced dots. Key: "∗", identical sequence; ":", conserved substitutions; ".", semiconserved substitutions (*49*). The nucleotide sequence of ENOX1 is available from GenBank under accession number EF432052.

The MBP-tagged cENOX1 and pMAL-c2E vector proteins were purified by using an amylose resin column. The MBP tag was then removed by digesting the MBP-tagged cENOX1 (lane 1) with TEV protease (Figure 8 inset). Upon treatment with TEV protease, both the native cENOX1 (71 kDa) and the MBP tag (43 kDa) were recovered (lane 2). The native cENOX1 formed insoluble aggregates and precipitated.

Aggregation and Electron Microscopy. Both the NusA-cENOX1 (MW 138 kDa) and the MBP cENOX1 after removal of the MBP tag formed insoluble and enzymatically inactive aggregates which were collected by centrifugation (Figure 8). Electron microscopic examination after negative staining with uranyl acetate revealed amorphous aggregates with occasional interspersed 10 nm diameter linear fibrils 100−200 nm long. The aggregated preparations lacked enzymatic activity and were refractory to resolubilization. The supernatants following centrifugation to remove aggregates lacked the structures as did vector proteins alone prepared under identical conditions.

Copper Binding and Site-Directed Mutagenesis of Potential Copper-Binding Sites. Several motifs were identified as potential copper-binding sites. They were HCKSC120, H260YSEH, Y304SM, H531SH, H579VH, and M608LLM. C120, H260, Y304, H531, H579, and M608 were individually replaced by alanines. The mutant MBP-tagged proteins were assayed for activities of NADH oxidation (Table 2). The wild-type MBP-tagged cENOX1 was the control. Mutations in H260YSEH or H579VH resulted in loss of

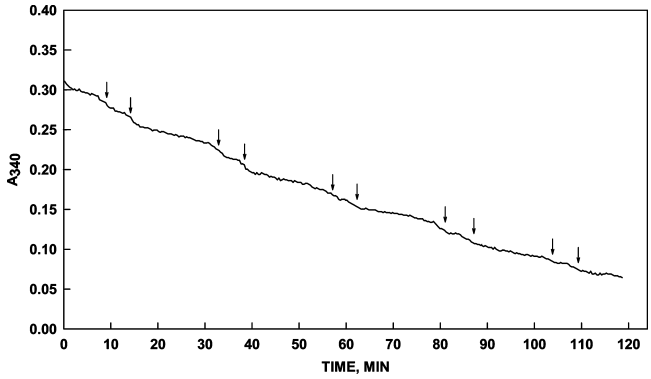

FIGURE 2: Continuous trace showing the decrease in A_{340} as a measure of consumption of NADH over 12 min for a fraction of IEF-purified MBP-tagged cENOX1. The assay conditions were as described ((*50*); see Methods) except that the NADH concentration was 0.75 mM and the data were collected automatically and stored using a SPECTRA max 340PC microplate reader. The mixture contained ca. 20 μg of MBP-tagged cENOX1 in a total volume of 200 μL.

NADH oxdiase activities. Both H260YSEH and H579VH when mutated in the same protein also produced a product with no activity.

For measurement of copper binding, the requirement for purified protein lacking an interfering tag was met by expressing cENOX1 carrying a maltose binding protein (MBP) tag by ligation of the cENOX1 DNA into the pMAL-c2E vector. After the pMAL-c2E vector protein, MBP-tagged cENOX1 protein and mutant MBP-tagged cENOX1 proteins were purified by amylose resin column chromatography; the copper amounts bound by each were measured by colorimetric assay with vector protein as control. The cENOX1 protein bound 2 mol of copper/mol of protein (Table 3). After either of the two copper-binding motifs was mutated, ca. 1 mol of copper/mol of protein was bound. When both copper-binding motifs were mutated, <1 mol of copper/mol of protein was bound (Table 3).

DISCUSSION

Querying ENOX2 sequence against databases revealed (along with orthologous proteins in different Vertebrata species) a group of paralogous proteins referred to as proliferation-inducing gene 38 proteins. In the human genome, the gene is located on the chromosome 13 (13q 14.11) and codes an open reading of 643 amino acids long (*28*). The sequences of the proliferation-inducing gene 38 protein appeared to be highly similar to that of ENOX2 (64% identity and 80% similarity in human) (Figure 1). A gene coding for the proliferation-inducing gene 38 protein is present in genomes of all so far sequenced Vertebrata and insect species. Like ENOX2, the protein is highly conserved (data not shown). In Mammalia with the XY system of sex determination the gene has autosomal localization in contrast to the ENOX2 coding gene which is located on the X chromosome in these species. For both proteins, the UniGene database contains multiple data confirming their expression (presence of mRNA) in a variety of species and tissues and at different developmental stages of different species. No similarity to either ENOX2 or the PIG 38 protein was found in plants, yeast, or prokaryotes. In the human, putative NADH-binding site, a disulfide−thiol interchange site and copper-binding sites of ENOX2 are also conserved in the proliferation-inducing gene 38 protein while the putative anticancer drug-binding site is not (Figure 1). This allows for consideration of the proliferation-inducing gene 38 protein as a putative ENOX1.

Sequencing of two clones of pET43.1a-cENOX1 revealed a new isoform of the human proliferation-inducing gene 38 protein having a semiconserved mutation of E16 to D. A homologous protein in *Danio rerio* also has D in this position. Homologues in *Equus caballus* and *Canis lupus familiaris* have another semiconserved substitution (E to Q) in this position, while in other species the E is conserved. The single nucleotide polymorphism (SNP) database contains more than 1000 entries for the human proliferation-inducing gene 38, but most of them are located in introns and do not affect the protein. Only a few indications of possible isoforms of human proliferation-inducing gene 38 protein were found. We are unaware of published information relating specifically to the function of the protein product of the proliferation-inducing gene 38.

Based on the high level of its similarity to ENOX2, the 71 kDa proliferation-inducing gene 38 protein was designated as cENOX1 (for candidate constitutive ECTO-NOX protein) (see Hugo Gene Nomenclature Committee Designation (http://www.gene.ucl.ac.uk/nomenclature/) for ENOX terminology) similar to the proliferating-inducing gene 38 protein (Figure 1). The protein was cloned and expressed in *E. coli* (NCBI accession number for the protein is AB028524).

When expressed in bacteria with a NusA tag, cENOX1 had activity characteristics of ENOX1 proteins from other mammalian (*1, 11, 29*) or plant (*1, 30*−*32*) sources. Activity measured either as NADH oxidation (artificial substrate) or oxidation of reduced coenzyme Q (native substrate) oscillated with five activity maxima within each 24 min period. Period length was determined from two major activity maxima separated by 6 min and indicated by single arrows in the figures. Other maxima were separated from each other and from the two major activity maxima by intervals of 4.5 min (6 min + 4 × 4.5 min = 24 min). The 24 min period length is distinct from the 22 min period length of ENOX2 (*22, 23*) and the 26 min period length of arNOX (*12, 13*).

The period of cENOX1 is phased by addition of melatonin as has been reported for ENOX1 proteins from other sources (*33*). Upon addition of melatonin, a new period occurs exactly 24 min after melatonin addition and continues with the newly established period thereafter. This is a characteristic not shared with either ENOX2 or arNOX. Also identifying the cENOX1 as an ENOX1 protein is its inability to be inhibited by the ENOX2 inhibitor capsaicin and other ENOX2 inhibitors including EGCg, phenoxodiol, and cisplatinum. This is consistent with the absence of the putative drug-binding site of ENOX2 (*22*).

Finally, the activity was inhibited by a polyclonal antibody raised to ENOX1 from human sera (*11*). ENOX2 antibodies had no effect on the cENOX1 activity (data not shown) nor did the ENOX1 antisera inhibit ENOX2 activity.

We are unable to exclude the possibility that additional ENOX1 proteins may be discovered with sequence substantially different from the cENOX1 reported here. Thus far, a number of these proteins have been purified to homogeneity but have failed to yield N-terminal amino acid sequence due to being blocked to N-terminal se-

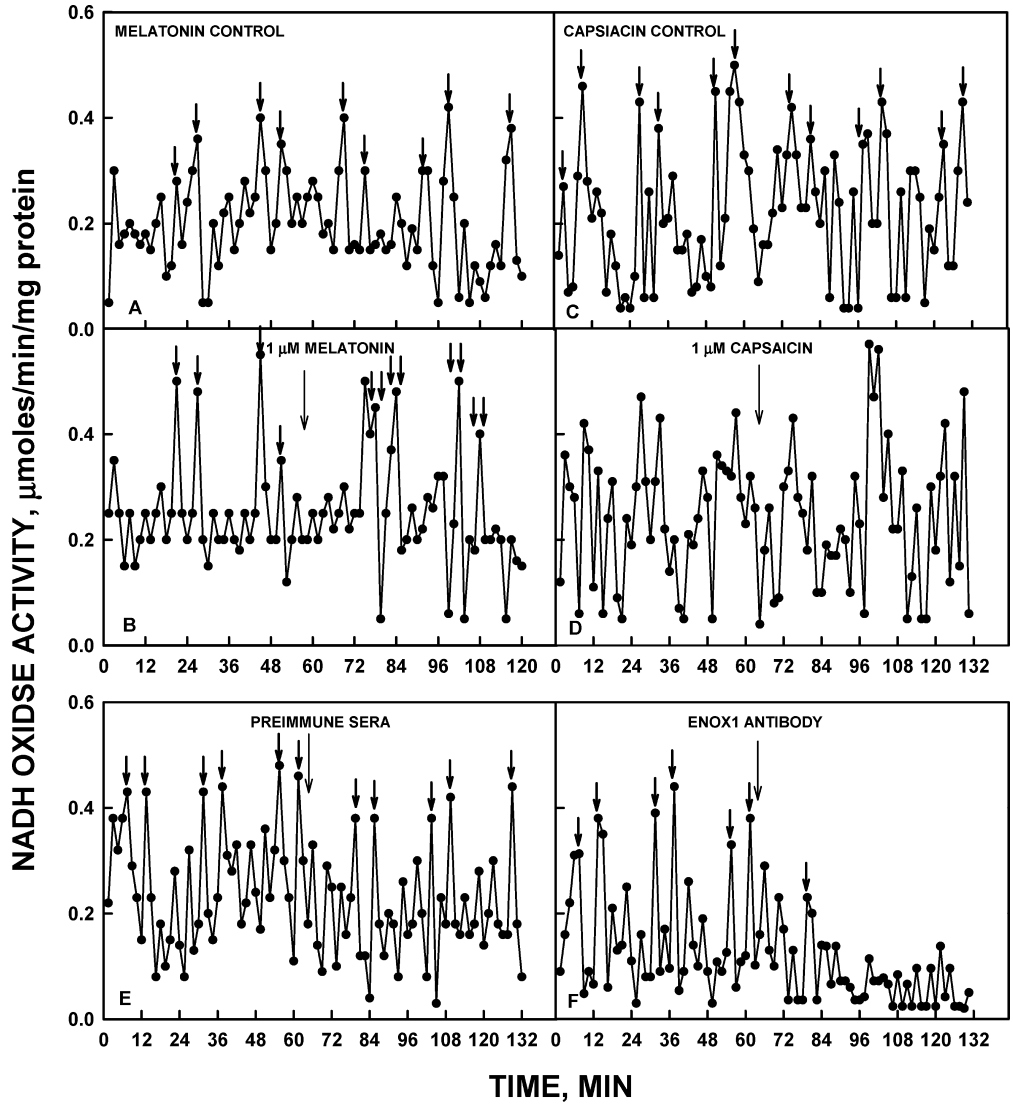

FIGURE 3: NADH oxidase activity of recombinant cENOX1 with a NusA tag and response to 1 μM melatonin (A, B), 1 μM capsaicin (C, D), and anti-human ENOX1 antibody (1:1000) (E, F) added where indicated at the large arrows in panels B, D, and F, respectively. In panel D, the response of recombinant ENOX2 to capsaicin (open circles, dotted lines) is included for comparison. For each treatment two assays were carried out simultaneously in parallel using paired Hitachi spectrophotometers with aliquots of the same cENOX1 preparation. Illustrated is the oscillatory pattern of five maxima. The major maxima separated by 6 min are indicated by single arrows. The three minor maxima that follow are separated from the major maxima and each other by 4.5 min creating the 24 min period ($6 + 4.5 \times 4 = 24$). Maxima appear at the same times comparing panels A and B prior to melatonin addition, panels C and D prior to capsaicin addition, and panels E and F prior to antibody addition illustrating the reproducibility of the oscillatory patterns. After addition of melatonin in panel B, new maxima appear 24 min following melatonin addition (double arrows), an ENOX1 characteristic. Capsaicin, a standard ENOX2 inhibitor, had no effect in panel D, and the activity was inhibited after one cycle in panel F by the addition of ENOX1 antibody.

quencing and being resistant to proteolytic degradation including proteinase K. Like ENOX2 (*34, 35*), the ENOX1 proteins share characteristics in common with prions (*36, 37*), Alzheimers Aβ protein (*38*), and aggregated tNOX proteins (*39*) especially those properties of resistance to protease degradation and the ability to aggregate. The aggregated preparations of cENOX1 lacked enzymatic activity and were refractory to resolubilization. Size exclusion chromatography revealed approximately 10% dimers, <2.5% monomers, and low molecular weight fragments with the remainder consisting of aggregates in the range of 250000 to >1000000 kDa. The cENOX2 aggregates while insoluble even in SDS were completely disaggregated by boiling in SDS not unlike amyloid-β (1−42), for example (*40*). For reasons possibly related to dimerization rather than multimerization, cENOX1 proteins prepared by isoelectric focusing or eluted from isoelectric focusing gels did not aggregate, retained enzymatic activity, and were stable in solution for several weeks or months stored frozen or at 4 °C.

An important consideration from the studies reported here is that the cENOX1 protein bound approximately 2 mol of copper/mol of protein. As the prevailing soluble form of ENOX2 proteins may be a dimer based on size exclusion chromatography, the presence of two coppers per monomer permits the ENOX1 to be viewed as a dimeric protein containing four coppers per dimer that is capable of carrying out four electron transfers from NADH or reduced coenzyme Q directly to molecular oxygen as required to form water. ENOX proteins do reduce molecular oxygen to water (*41*) despite the fact that they lack flavin and/or electron carriers other than copper (*22*).

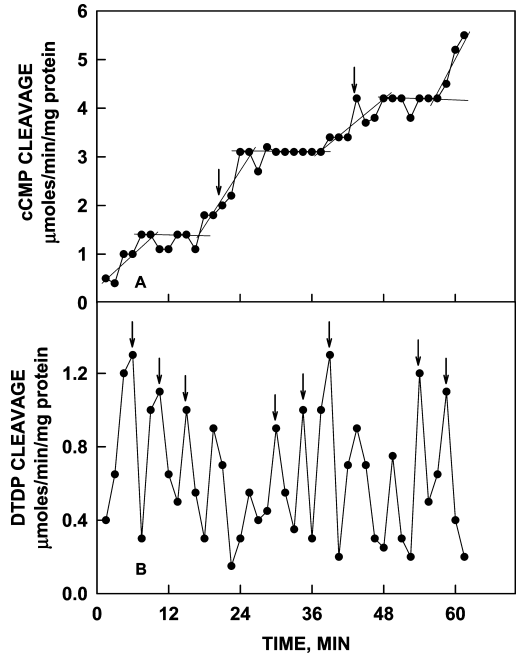

FIGURE 4: Protein disulfide−thiol interchange activity of NusA-tagged cENOX1 measured from the activation of the ability of scrambled and inactive RNase to cleave cCMP measured spectrophotometrically (A) or determined by cleavage of a dithiodipyridine (DTDP) substrate (B). Both activities exhibited an oscillatory activity. However, the activities were most strongly associated with the three maxima separated by 4.5 min rather than with the two maxima separated by 6 min.

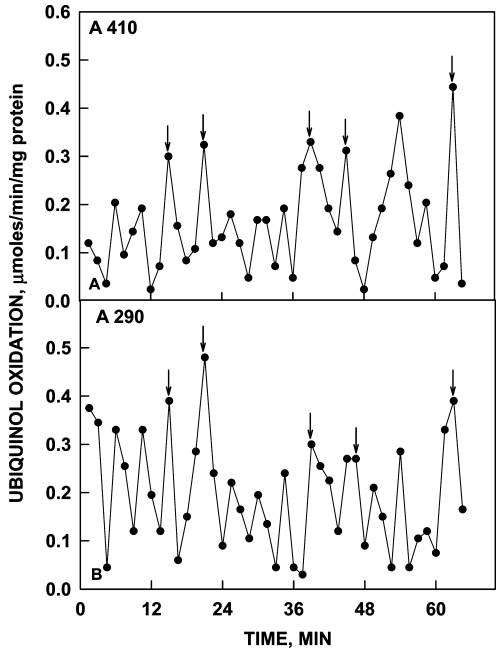

FIGURE 5: Ability of recombinant NusA-tagged cENOX1 to oxidize hydroquinone (reduced coenzyme Q) measured either by an increase in A_{410} (A) or by a decrease in A_{290} (B). As with NADH oxidation of Figure 3, the activity oscillates with prominent maxima separated by 6 min (arrows) to create a 24 min period containing three additional maxima separated by 4.5 min (total of five maxima).

This protein disulfide isomerase-like activity measured either as restoration of activity to denatured and inactive ribonuclease A or by cleavage of dithiodipyridine (DTDP) substrate also exhibits the oscillatory activity patterns characteristic of ENOX proteins in general. For cENOX1 the period length was again 24 min due to the asymmetry

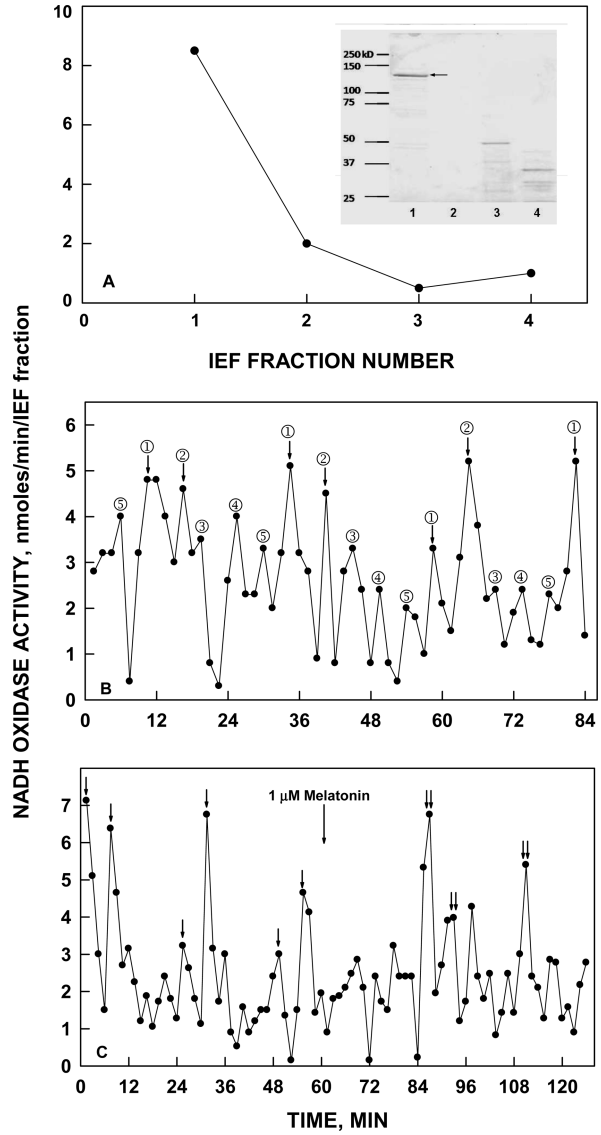

FIGURE 6: Purification of recombinant NusA-tagged cENOX1 protein by isoelectric focusing and assay of eluted fractions. (A) Assay of recombinant NusA-tagged cENOX1 activity eluted from slices of an isoelectric focusing gel in which the activity correlated with the position of the protein on the gel. The inset shows silver staining analysis of the SDS−PAGE gel for NusA-tagged cENOX1 protein fractions eluted from the isoelectric focusing gel. Lane 1: NusA-cENOX 1 protein fraction eluted from p*I* 7−10 gel slice (IEF fraction 1). Lane 2: Protein fraction eluted from p*I* 6−7 gel slice (IEF fraction 2). Lane 3: Protein fraction eluted from p*I* 4.5−6 gel slice (IEF fraction 3). Lane 4: Protein fraction eluted from p*I* 3−4.5 gel slice (IEF fraction 4). (B, C) NADH oxidase activity of gel slices corresponding to the position of 138 kDa NusA-tagged cENOX1 (arrow, IEF fraction 1 of panel A inset). Other gel regions were without activity. The characteristic oscillatory pattern in panel B was observed, and in panel C, the phase of the activity oscillations was shifted by addition of 1 μM melatonin (double arrows).

imparted by two of the five maxima per period being separated by 6 min rather than the usual 4.5 min. The protein disulfide−thiol interchange activity of the ENOX protein has been implicated as obligatory to the cell enlargement phase of cell growth for both animal (*10, 14*) and plant (*15, 16*) cells. However, the mechanism whereby disulfide bonds are formed and broken through the action of NOX proteins may differ substantially from that of the classical flavoprotein disulfide isomerases. The portion of the cENOX1 protein involved in protein disulfide−thiol interchange is unknown.

Table 1: NADH Oxidase Activity of IEF-Purified NusA-Tagged cENOX1 and Response to ENOX2 Inhibitors and the ENOX1 Inhibitor Simalikalactone D[a]

inhibitor	μmol min^{-1} mg^{-1}
none	0.43 ± 0.07
cis-platinum (100 μM)	0.42 ± 0.06
phenoxodiol (10 μM)	0.41 ± 0.06
EGCg (500 μM)	0.46 ± 0.07
capsaicin (1 μM)	0.43 ± 0.06
simalikalactone D (1 μM)	0.08 ± 0.01

[a] Average of three determinations ± standard deviations. The concentrations of cis-platinum, phenoxodiol, EGCg, and capsaicin used results in >90% inhibition of recombinant NusA-tagged ENOX2 assayed in parallel (e.g., Figure 3D).

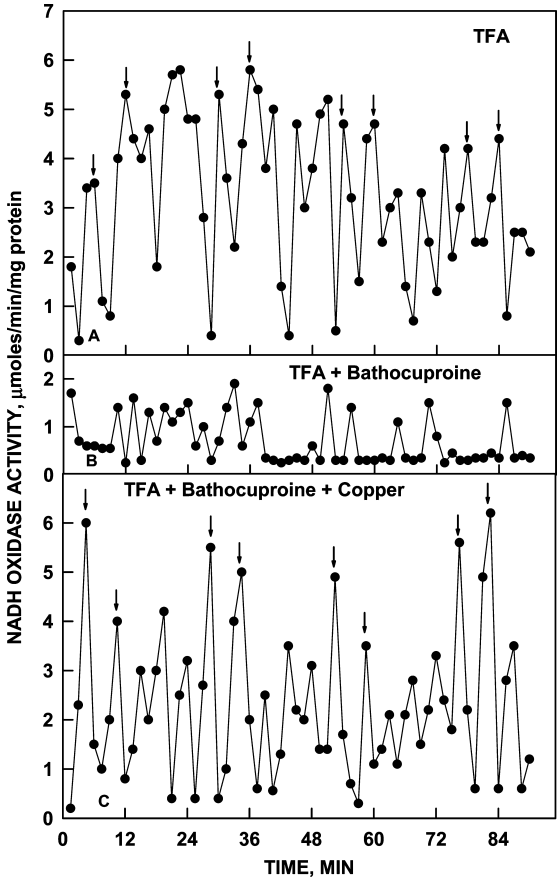

FIGURE 7: Recombinant MBP-tagged cENOX1 activity eluted from an IEF gel was unfolded by treatment with trifluoroacetic acid (TFA) in the absence (A) or presence (B) of 0.3 mM bathocuproine to remove copper. Following dialysis to remove the bathocuproine and the TFA, an oscillatory activity was restored in the absence of bathocuproine (A) but was lost or reduced in its presence (B). Activity to panel B was restored by refolding in the presence of 100 μM copper chloride at physiological pH (C).

ENOX proteins contain only one of the two -CXXC- motifs characteristic of the flavin-containing protein disulfide isomerases (ref *22*; Figure 3). A CKSC120A replacement in cENOX1 did not result in loss of activity but changed the length of the oscillatory period from 24 to 30 min. Additionally, a 34 kDa ENOX2 processed form lacking the -CXXC- motif entirely exhibits full protein disulfide−thiol interchange activity. A source of protons and electrons is not required for the interchange activity as exemplified by the ability of cENOX1 alone to catalyze the restoration of activity to inactive and denatured ribonuclease A. Furthermore, NOX proteins are not thioredoxin reductases and

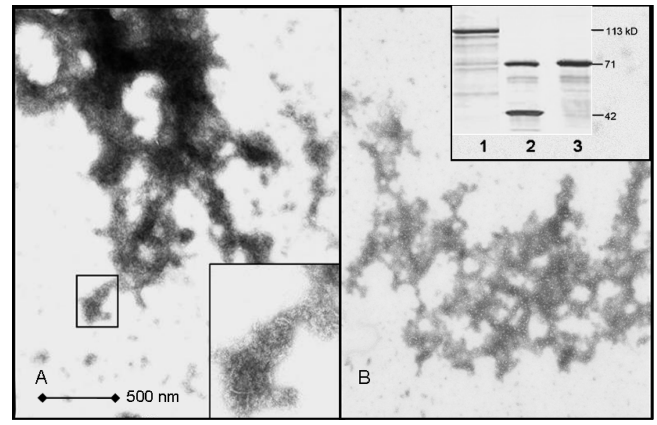

FIGURE 8: Aggregated and precipitated cENOX1 analyzed by electron microscopy for NasA-tagged cENOX1 before (A) and MBP-tagged cENOX1 after tag removal. The inset in panel B shows a silver-stained SDS−PAGE gel of undigested and digested MBP-tagged cENOX1 proteins. Lane 1: MBP-tagged CENOX (113 kDa). Lane 2: Digested recombinant protein solution containing MBP (42 kDa) and cENOX (71 kDa). Lane 3: Precipitated cENOX after ultracentrifugation.

Table 2: NADH Oxidase Specific Activities of Mutated Recombinant MBP-Tagged cENOX1 To Identify Copper-Binding Sites[a]

protein	*N*	μmol min^{-1} mg^{-1}
WT	18	0.40 ± 0.03
C120A	9	0.36 ± 0.07
H260A	3	0.05 ± 0.05[b]
Y304A	3	0.37 ± 0.09
H531A	6	0.50 ± 0.03[b]
H579A	9	0.07 ± 0.09[b]
M608A	3	0.03 ± 0.03
H260A + H579A	3	0.05 ± 0.05[b]

[a] The activity of the vector protein (0.005 ± 0.002 μmol min^{-1} mg^{-1}) was subtracted as background. [b] Significantly different from wild type (WT), $p < 0.001$.

Table 3: Bound Copper Comparing MBP-Tagged cENOX1, Mutant MBP-cENOX1, and pMAL-c2E Vector Protein

	protein (μM)	copper (μM)	ratio[a]
pMAL-c2E vector	25.49 ± 2.02	5.80 ± 1.76	0.22 ± 0.06[c]
MBP-cENOX1	10.60 ± 1.17	21.07 ± 3.85	1.98 ± 0.14[a]
MBP-cENOX H260A	9.38 ± 1.92	12.38 ± 1.62	1.33 ± 0.10[b]
MBP-cENXO1 H579A	9.44 ± 1.31	10.60 ± 1.42	1.14 ± 0.27[b]
MBP-cENXO1 H260A + H579A	8.75 ± 1.61	4.76 ± 0.92	0.56 ± 0.17[c]

[a] By comparing five means of ratios using statistic adjustment under analysis of variance (ANOVA), a, b, and c are groups of ratios within which the means are not significantly different from each other at $\alpha = 0.05$. However, between groups of a, b, and c there are significant differences at $\alpha = 0.05$.

neither glutathione nor dithiothreitol support the protein disulfide−thiol interchange activity.

The high capacity of proliferating mammalian cells to transfer electrons from cytosolic NADH to extracellular acceptors like oxygen is poorly understood and not readily recognized (*42, 43*). Yet cells have been shown to consume oxygen at the cell surface via a plasma membrane electron transport chain involving coenzyme Q as the transmembrane carrier of electrons and protons (*44*−*46*). It is of interest in this regard that Scarlett et al. (*47*) first identified an approximately 70 kDa plasma membrane protein of human 143B osterosarcoma cells by polyacrylamide gel electrophoresis that reacted on Western blots with our CNOX

antisera. In this context, the identification and cloning of the candidate constitutive ENOX protein whose proposed function is as a terminal oxidase for the plasma membrane electron transport chain (*44*), rather than superoxide generation (*48*), represent an important advance in our understanding of the enzyme proteins involved in plasma membrane electron transport which, until recently, have been largely ill-defined (*45*).

ACKNOWLEDGMENT

We thank Dr. Debra Sherman and the Life Sciences Microscopy Facility of Purdue University for electron microscopy, Nicole Weston for figure preparation, Lian-Ying Wu for cell culture, and the laboratory of Prof. Carol Post for advice, helpful discussions, access to laboratory personnel, and use of equipment and facilities. The similarity searches and analyses and the design of primers for cloning cENOX1 as an MBP-fused protein were contributed by Nina Gorenstein.

REFERENCES

1. Morré, D. J. (1998) NADH oxidase: a multifunctional ectoprotein of the eukaryotic cell surface, in *Plasma Membrane Redox Systems and Their Role in Biological Stress and Disease* (Asard, H., Bérczi, A., and Caubergs, R., Eds.) pp 121−156, Kluwer Academic Publishers, Dordrecht, The Netherlands.
2. Morré, D. J., and Morré, D. M. (2003) Cell surface NADH oxidases (ECTO-NOX proteins) with roles in cancer, cellular time-keeping, growth, aging and neurodegenerative disease. *Free Radical Res. 37*, 795–808.
3. Morré, D. J., Chueh, P.-J., and Morré, D. M. (1995) Capsaicin inhibits preferentially the NADH oxidase and growth of transformed cells in culture. *Proc. Natl. Acad. Sci. U.S.A. 92*, 1831–1835.
4. Morré, D. J., Sun, E., Geilen, C., Wu, L.-Y., de Cabo, R., Krasagakis, K., Orfanos, C. E., and Morré, D. M. (1996) Capsaicin inhibits plasma membrane NADH oxidase and growth of human and mouse melanoma lines. *Eur. J. Cancer 32A*, 1995–2003.
5. Morré, D. J., Wu, L.-Y., and Morré, D. M. (1995) The antitumor sulfonylurea N-(4-methylphenylsulfonyl)-N-(chlorophenyl)urea (LY181984) inhibits NADH oxidase activity of HeLa plasma membranes. *Biochim. Biophys. Acta 1240*, 11–17.
6. Morré, D. J., Wilkinson, F. E., Kim, C., Cho, N., Lawrence, J., Morré, D. M., and McClure, D. (1996) Antitumor sulfonylurea-inhibited NADH oxidase of cultured HeLa cells shed into media. *Biochim. Biophys. Acta 1280*, 197–206.
7. Wilkinson, F. E., Kim, C., Cho, N., Chueh, P.-J., Leslie, S., Moya-Camarena, S., Wu, L.-Y., Morré, D. M., and Morré, D. J. (1996) Isolation and identification of a protein with capsaicin-inhibited NADH oxidase activity from culture media conditioned by growth of HeLa cells. *Arch. Biochem. Biophys. 336*, 275–282.
8. Chueh, P.-J., Morré, D. J., Wilkinson, F. E., Gibson, J., and Morré, D. M. (1997) A 33.5 kDa heat- and protease-resistant NADH oxidase inhibited by capsaicin from sera of cancer patients. *Arch. Biochem. Biophys. 342*, 38–47.
9. Morré, D. J., Caldwell, S., Mayorga, A., Wu, L.-Y., and Morré, D. M. (1997) NADH oxidase activity from sera altered by capsaicin is widely distributed among cancer patients. *Arch. Biochem. Biophys. 342*, 224–230.
10. Wang, S., Pogue, R., Morré, D. M., and Morré, D. J. (2001) NADH oxidase activity (NOX) and enlargement of HeLa cells oscillate with two different temperature-compensated period lengths of 22 and 24 minutes corresponding to different NOX forms. *Biochim. Biophys. Acta 1539*, 192–204.
11. Sedlak, D., Morré, D. M., and Morré, D. J. (2001) A drug-unresponsive and protease-resistant CNOX protein from human sera. *Arch. Biochem. Biophys. 386*, 106–116.
12. Morré, D. M., and Morré, D. J. (2003) Specificity of coenzyme Q inhibition of an aging-related cell surface NADH oxidase (ECTO-NOX) that generates superoxide. *BioFactors 18*, 33–43.
13. Morré, D. M., Guo, F., and Morré, D. J. (2003) An aging-related cell surface NADH oxidase (arNOX) generates superoxide and is inhibited by coenzyme Q. *Mol. Cell. Biochem. 254*, 101–109.
14. Pogue, R., Morré, D. M., and Morré, D. J. (2000) CHO cell enlargement oscillates with a temperature-compensated period of 24 minutes. *Biochim. Biophys. Acta 1498*, 44–51.
15. Morré, D. J., Pogue, R., and Morré, D. M. (2001) Soybean cell enlargement oscillates with a temperature-compensated period length of ca. 24 min. *In Vitro Cell. Dev. Biol.: Plant 37*, 19–23.
16. Morré, D. J., Ternes, P., and Morré, D. M. (2002) Cell enlargement of plant tissue explants oscillates with a temperature-compensated period length of ca. 24 min. *In Vitro Cell. Dev. Biol.: Plant 38*, 18–28.
17. Morré, D. J., Brightman, A. O., Hidalgo, A., and Navas, P. (1995) Selective inhibition of auxin-stimulated NADH oxidase activity and elongation growth of soybean hypocotyls by thiol reagents. *Plant Phys. 107*, 1285–1291.
18. Morré, D. J., and Greico, P. A. (1999) Glaucarubolone and simalikalactone D, respectively, preferentially inhibit auxin-induced and constitutive components of plant cell enlargement and the plasma membrane NADH oxidase. *Int. J. Plant Sci. 160*, 291–297.
19. Kishi, T., Morré, D. M., and Morré, D. J. (1999) The plasma membrane NADH oxidase of HeLa cells has hydroquinone oxidase activity. *Biochim. Biophys. Acta 1412*, 66–77.
20. Morré, D. J., De Cabo, R., Jacobs, E., and Morré, D. M. (1995) Auxin-modulated protein disulfide-thiol interchange activity from soybean plasma membranes. *Plant Physiol. 109*, 573–578.
21. Morré, D. J., Gomez-Rey, M. L., Schramke, C., Em, O., Lawler, J., Hobeck, J., and Morré, D. M. (1999) Use of dipyridyl-dithio substrates to measure directly the protein disulfide-thiol interchange activity of the auxin stimulated NADH:protein disulfide reductase (NADH oxidase) of soybean plasma membranes. *Mol. Cell. Biochem. 200*, 7–13.
22. Chueh, P.-J., Kim, C., Cho, N., Morré, D. M., and Morré, D. J. (2002) Molecular cloning and characterization of a tumor-associated, growth-related and time-keeping hydroquinone (NADH) oxidase (NOX) of the HeLa cell surface. *Biochemistry 41*, 3732–3741.
23. Morré, D. J., Chueh, P.-J., Pletcher, J., Tang, X. Y., Wu, L.-Y., and Morré, D. M. (2002) Biochemical basis for the biological clock. *Biochemistry 41*, 11941–11945.
24. Chueh, P.-J., Morré, D. M., and Morré, D. J. (2002) A site-directed mutagenesis analysis of tNOX functional domains. *Biochim. Biophys. Acta 1594*, 74–83.
25. Altschul, S. F., Madden, T. L., Schäffer, A. A., Zhang, J., Zhang, Z., Miller, W., and Lipman, D. J. (1997) Gapped BLAST and PSI-BLAST: a new generation of protein database search programs. *Nucleic Acids Res. 25*, 3389–3402.
26. Smith, P. K., Krohn, R. I., Hermanson, G. T., Mailia, A. K., Gartner, F. F., Provenzano, M. D., Fujimoto, E. K., Groeke, N. M., Olson, B. J., and Klenk, D. C. (1985) Measurement of proteinusing bicinchoninic acid. *Anal. Biochem. 150*, 70.
27. Brenner, A. J., and Harris, E. D. (1995) A quantitative test for copper using bicinchoninic acid. *Anal. Biochem. 226*, 80–84.
28. Venter, J. C., et al. (2001) The sequence of the human genome. *Science 291*, 1304–1351.
29. Brightman, A. O., Wang, J., Miu, R. K., Sun, I. L., Barr, R., Crane, F. L., and Morré, D. J. (1992) A growth factor- and hormone-stimulated NADH oxidase from rat liver plasma membrane. *Biochim. Biophys. Acta 1105*, 109–117.
30. Morré, D. J., and Brightman, A. O. (1991) NADH oxidase of plasma membranes. *J. Bioenerg. Biomembr. 23*, 469–489.
31. Brightman, A. O., Barr, R., Crane, F. L., and Morré, D. J. (1988) Auxin-stimulated NADH oxidase purified from plasma membrane of soybean. *Plant Physiol. 86*, 1264–1269.
32. Morré, D. J., and Morré, D. M. (1998) NADH oxidase activity of soybean plasma membrane oscillates with a temperature compensated period of 24 min. *Plant J. 16*, 279–284.
33. Morré, D. J., Penel, C., Greppin, H., and Morré, D. M. (2002) The plasma membrane-associated NADH oxidase of spinach leaves responds to blue light. *Int. J. Plant Sci. 613*, 543–547.
34. Kelker, M., Kim, C., Chueh, P. J., Guimont, R., Morré, D. M., and Morré, D. J. (2001) Cancer isoform of a tumor-associated cell surface NADH oxidase (tNOX) has properties of a prion. *Biochemistry 40*, 7351–7354.
35. Kim, C., and Morré, D. J. (2004) Prion proteins and ECTO-NOX proteins exhibit similar oscillating redox activities. *Biochem. Biophys. Res. Commun. 315*, 1140–1146.

36. Griffith, J. S. (1964) Self-replication and scrapie. *Nature 315*, 1043–1044.
37. Prusiner, S. B. (1994) Biology and genetics of prion diseases. *Annu. Rev. Microbiol. 48*, 655–686.
38. Multhaup, G. (1997) Amyloid precursor protein, copper and Alzheimer's disease. *Biomed. Pharmacother. 51*, 105–111.
39. del Castillo-Olivares, A., Yantiri, F., Chueh, P.-J., Wang, S., Sweeting, M., Sedlak, D., Morré, D. M., Burgess, J., and Morré, D. J. (1998) A drug-responsive and protease-resistant peripheral NADH oxidase complex from the surface of HeLa S cells. *Arch. Biochem. Biophys. 358*, 125–140.
40. Rangachari, V., Moore, B. D., Reed, D. K., Sonoda, L. K., Bridges, A. W., Conboy, E., Hartigan, D., and Rosenberry, T. L. (2007) Amyloid-β (1−42) rapidly forms protofibrils and oligomers by distinct pathways in low concentrations of sodium dodecyl sulfate. *Biochemistry 46*, 12451–12462.
41. Orczyk, J., Morré, D. M., and Morré, D. J. (2005) Periodic fluctuations in oxygen consumption comparing HeLa (cancer) and CHO (non-cancer) cells and response to external NAD(P)$^+$/NAD(P)H. *Mol. Cell. Biochem. 273*, 161–167.
42. Berridge, M. V., and Tan, A. S. (2000) High-capacity redox control at the plasma membrane of mammalian cells: trans-membrane, cell surface, and serum NADH-oxidases. *Antioxid. Redox Signaling 2*, 231–242.
43. Hyun, D.-H., Hunt, N. D., Emerson, S. S., Hernandez, J. O., Mattson, M. P., and de Cabo, R. (2007) Up-regulation of plasma membrane-associated redox activities in neuronal cells lacking functional mitochondria. *J. Neurochem. 100*, 1364–1374.
44. Crane, F. L., and Low, H. (2008) Reactive oxygen species generation at the plasma membrane for antibody control. *Autoimmun. Rev. 7*, 518–522.
45. Baker, M. A., and Lawen, A. (2000) Plasma membrane NADH-oxidoreductase system: A critical review of the structural and functional data. *Antioxid. Redox Signaling 2*, 197–212.
46. Herst, P. M., and Berridge, M. V. (2006) Plasma membrane electron transport: A new target for cancer drug development. *Curr. Mol. Med. 6*, 895–904.
47. Scarlett, D.-J. G., Herst, P. M., and Berridge, M. V. (2005) Multiple proteins with single activities or a single protein with multiple activities: The conundrum of cell surface NADH oxidoreductases. *Biochim. Biophys. Acta 1708*, 108–119.
48. Morré, D. M., Guo, F., and Morré, D. J. (2003) An aging-related cell surface NADH oxidase (arNOX) generates superoxide and is inhibited by coenzyme Q. *Mol. Cell. Biochem. 254*, 101–109.
49. Larkin, M. A., Blackshields, G., Brown, N. P., Chenna, R., McGettigan, P. A., McWilliam, H., Valentin, F., Wallache, I. M., Wilm, A., Lopez, R., Thompson, J. D., Gibson, T. J., and Higgins, D. G. (2007) ClustalW and ClustalX version 2. *Bioinformatics 23*, 2947–2948.
50. Morré, D. J., and Morré, D. M. (2003) Spectroscopic analyses of oscillations in ECTO-NOX-catalyzed oxidation of NADH. *Nonlinearity Biol. Toxicol. Med. 1*, 345–362.

BI801073P